Aromaticity versus Regioisomeric Effect of β-Substituents in Porphyrinoids

Journal:	*Physical Chemistry Chemical Physics*
Manuscript ID	CP-ART-02-2019-001177.R1
Article Type:	Paper
Date Submitted by the Author:	09-Apr-2019
Complete List of Authors:	Yao, Yuhang; Peking University Rao, Yu; Peking University Liu, Yi-Wei; Peking University, College of Chemistry and Molecular Engineering Jiang, Liang; Nanjing University Xiong, Jin; Peking University Fan, Ying-Jie; Peking University Shen, Zhen; Nanjing University Sessler, Jonathan; University of Texas at Austin Zhang, Jun-Long; Peking University, Chemistry

Journal Name

ARTICLE

Aromaticity *versus* Regioisomeric Effect of *β*-Substituents in Porphyrinoids

Received 00th January 20xx,
Accepted 00th January 20xx

DOI: 10.1039/x0xx00000x

www.rsc.org/

Yuhang Yao,[†,§] Yu Rao,[†,§] Yiwei Liu,[†] Liang Jiang,[‡] Jin Xiong,[†] Ying-Jie Fan,[†] Zhen Shen,*[‡] Jonathan L. Sessler*[,#,Δ] and Jun-Long Zhang*[,†]

The photophysical properties of naturally occurring chlorophylls depend on the regioisomeric nature of the *β*-pyrrolic substituents. Such systems are the "gold standard" by which such effects are judged. However, simple extrapolations from what have been learned with chlorophylls may not be appropriate for other partially reduced porphyrinoids. Here we report the synthesis of a series of *cis*/*trans*-porphodilactones (*cis*/*trans*-**1**) and related derivatives (*cis*/*trans* **2**-**5**) designed to probe the effect of regioisomeric substitution in porphyrinoids that incorporate degrees of unsaturation through the *β*-pyrrolic periphery that exceed those of chlorophyll. These test systems were obtained through *β*-pyrrolic modifications of the tetrapyrrolic core, which included reduction of *β*-diazalone to the corresponding dilactol moieties and 1,3-dipolar cycloadditions. In the case of *cis*- vs. *trans*-**3** bearing two pyrrolidine-fused *β*-rings we found an unprecedented ΔQ_L up to ca. 71 nm (2086 cm^{-1}), where ΔQ_L (Q_L means the lowest energy transfer band, also the S_0->S_1 transition band, which is often assigned as $Q_y(0,0)$ band) refers to the transition energy difference between the corresponding *cis*/*trans*-isomers. The ΔQ_L values for these and other systems reported here were found to depend on the differences in the HOMO-LUMO energy gap and to be tied to the degeneracy and energy level splitting of the FMOs, as inferred from a combination of MCD spectral studies and DFT calculations. The aromaticity, estimated from the chemical shifts of the N-H protons and supported by theoretical calculations (e.g., AICD plots and NICS(1) values), was found to correlate with the extent of porphyrin periphery saturation resulting from the specific *β*-modifications. The aromaticity proved inversely proportional to the degree to which the regioisomerism affected the photophysical properties as noted from plots of ΔQ_Ls in cm^{-1} vs the average NICS(1) values for **1**-**5**. Such a finding is not something that can be easily interpolated from prior work and thus reveals how aromaticity may be used to fine-tune photophysical effects in reduced porphyrinoids.

Introduction

Regioisomeric effects, specifically where carbonyl substituents are placed on the *β*-pyrrolic periphery of unsaturated porphyrin derivatives, can have a profound effect on the electronic structures, photophysical properties, and intermolecular interactions of these quintessential π-conjugated chromophores.[1] The impact of these effects has recently come to be recognized in the context of organic optoelectronics.[2] They are also appreciated for the role they play in regulating the optical features of natural occurring tetrapyrroles. Likely, regioisomeric substitution effects play a key role in fine-tuning the biological features of these "life pigments", as exemplified by chlorophylls, such as *chl b*, *d*, and *f*, isolated from both the sea and the land.[1b, 1e, 3] For example, the lowest energy absorption difference, ΔQ_L, where ΔQ_L (Q_L means the lowest energy transfer band, also the S_0->S_1 transition band, which is often assigned as Qy(0,0) band) refers to the transition energy difference between the corresponding *cis*/*trans*-isomers, between *chl d* and *f* is 9 nm (183 cm^{-1}, Figure 1).[3f, 4] The origin of this difference is ascribed to the relative orientations of the formyl or vinyl substituents on the porphyrin periphery, and is viewed as a phenomenon that is well understood in the case of chlorophyll derivatives.[3] In fact, the effect could be recapitulated by Lindsey and co-workers through preparative work involving chlorins.[5] However, the regioisomeric consequences of *β*-pyrrolic substitution have been much less studied in the case of other porphyrinoids and seemingly contradictory findings have been reported in the literatures. For instance, as early as 1969 Inhoffen and co-workers reported the orientation of *β*-dioxo groups influenced the absorptions of dioxobacteriochlorin isomers (ΔQ_L= 18 nm, or 387 cm^{-1}, Figure 1).[6] In 1986, Chang et al. synthesized isomeric porphyrindiones with ketone groups in different orientations in adjacent pyrroles and found a ΔQ_L of 16 nm (403 cm^{-1}) between the isomers in their free-base forms.[7] In 1991, the same group reported that the ΔQ_L increased up to 71 nm (2086 cm^{-1}) upon coordination of copper(II) ion.[8] In a sharp contrast, in 2002 Cavaleiro, *et al.* observed,

[†]*Beijing National Laboratory for Molecular Sciences, State Key Laboratory of Rare Earth Materials Chemistry and Applications, College of Chemistry and Molecular Engineering, Peking University, Beijing 100871, P. R. China. E-mail: zhangjunlong@pku.edu.cn; Fax: +86-10-62767034.*
[‡]*State Key Laboratory of Coordination Chemistry, School of Chemistry and Chemical Engineering, Nanjing University, Nanjing 210093, P. R. China. E-mail: zshen@nju.edu.cn*
[#]*Institute for Supramolecular Chemistry and Catalysis, Shanghai University, Shanghai, 200444, P. R. China. E-mail: sessler@cm.utexas.edu*
[Δ]*Department of Chemistry, The University of Texas at Austin, Austin, Texas 78712-1224, USA*
[§]*These authors contributed equally to this work.*
† Electronic Supplementary Information (ESI) available: See DOI: 10.1039/x0xx00000x

Journal Name

ARTICLE

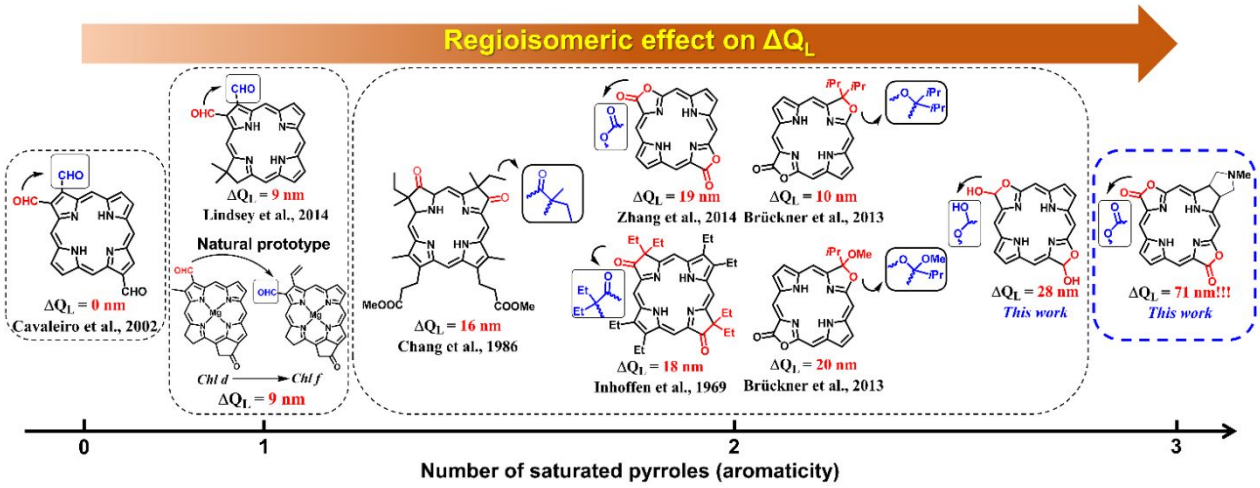

Figure 1. Families of porphyrinoid isomers grouped so as to show the how effect of substitution depends on the degree of aromaticity as reflected in the extent of *β*-pyrrolic saturation (*meso*-aryl groups omitted for clarity). The substitutions drawn by red and blue indicate the *cis* and *trans* isomers respectively, the lowest energy absorption difference (ΔQ_L) are listed, and the authors with the years of literature are also presented below the structures.

however, no difference in the absorption features of isomers that differed in terms of the orientation of two *β*-formyl groups on the periphery.[9] Later Brückner and we found that the *cis/trans*-porphodilactone isomers (*cis*/*trans*-**1**) and their derivatives, characterized by different orientations of the constituent *β*-diazalone moieties, displayed distinctively different absorption (ΔQ_L = 10-20 nm) and emission features.[10] This latter regioisomeric effect was reflected in the respective triplet energies.

Being able to fine-tune the electronic features through control of regioisomeric effects may allow for the production of chromophores optimized for a certain applications or better control over NIR lanthanide sensitization and triplet annihilation-based upconversion.[10a, 11] However, currently a clear understanding of the fundamental relationship between regioisomeric substitution effects and the photophysical properties of highly reduced tetrapyrrolic chromophores is lacking. The present study was instigated with the goal of obtaining such fundamental structure-function insights.

As a first step, we analysed the differences in the lowest energy absorption spectral maxima using sets of previously reported congeneric porphyrinoid regioisomers.[4-6, 9-10, 12] Although isomeric copper porphyrindiones showed the pronounced regioisomeric effect,[8] the unknown role of copper coordination renders difficult comparison with the most reported porphyrinoid free bases and thus we focused on the porphyrinoid free bases in the context. We noticed a possible inverse relationship between ΔQ_L and degree of saturation represented by the number of the saturated pyrroles (cf. Figure 1). Specifically, ΔQ_L was found to increase as the number of saturated *β*-pyrroles increased from 0 to 2. In an effort to confirm or refute the validity of this observation, we have prepared several new derivatives of the *cis/trans*-porphodilactones **1**, namely the isomeric lactols, *cis*/*trans*-**2**, the further tri-substituted pyrrole system *cis*/*trans*-**3**, and oxidized forms of the latter, viz. *cis*/*trans*-**4** and *cis*/*trans*-**5**. In accord with our preliminary expectations, the ΔQ_L values were found to increase as the saturation level of the *β*-periphery increased. In fact, an unprecedented ΔQ_L was observed (up to ca. 71 nm; 2086 cm^{-1}) for *cis*- vs *trans*-**3**. To our best of knowledge, this ΔQ_L is the largest in the porphyrinoid free base system. The present study was thus undertaken with a goal to understanding the effects of macrocyclic structure on the optical feature of porphyrinoid regioisomers. We note that pyrrocorphins and related corphinoids with three hydrogenated or saturated pyrroles were reported early on by Eschenmoser, Chang, and Cavaleiro and co-workers.[7, 13] However, their photophysical properties were not investigated in detail. Thus, an ancillary objective was to carry out fundamental studies that might provide further insights into these classic systems.

Results and Discussion

Synthesis and Characterization

The synthesis of *cis*/*trans*-**2**-**5** is summarised in Scheme 1. Starting from *cis*/*trans*-**1** and following Cavaleiro's procedure with slight modification,[13d, 14] *cis*- and *trans*-**3** were obtained in yields of 57 and

66%, respectively, through 1,3-dipolar cycloaddition of azomethine ylides. *Cis*/*trans*-**4** were then obtained by subjecting *cis*/*trans*-**3** to oxidation with 2,3-dichloro-5,6-dicyano-1,4-benzoquinone (DDQ) in toluene.[15] Further oxidation of *cis*/*trans*-**4** by oxygen under conditions of photo-irradiation produced *cis*/*trans*-**5** in 16 and 18% yield, respectively.[16] Separately *cis*/*trans*-**1** was subject to diisobutylaluminium hydride (DIBAL-H) reduction in THF, according to Brückner's procedure; this allowed us to obtain *cis*/*trans*-**2**.[10b, 17] However, attempts to reduce *cis*/*trans*-**3** to the corresponding porphodilactols proved unsuccessful. For instance, **3** was found to decompose in the presence of DIBAL-H. In addition, we only isolated one form of *cis* isomer in **3**-**5**, and this was analysed in the supporting information (Scheme S7).

The chemical shifts of the inner N-H signals seen in the ^{1}H NMR spectra of *cis*/*trans*-**1**-**5** were found to vary from -1.64 to 6.53 ppm. This was taken as evidence that there are significant differences in the ring currents within this series as a function of *β*-modification. It also provided an initial hint that aromaticity effects would prove important in terms of analysing the optical features (see discussion below). Detailed synthetic procedures and full characterization data are listed in the Experimental Section or the Supporting Information (Schemes S1-S6 and Figure S1-S40). All new compounds were fully characterized using ^{1}H, ^{13}C and ^{19}F NMR spectroscopies, mass spectrometry (MS), and infrared (IR) spectroscopy. In addition, 2D-NMR (COSY and NOSEY) experiments revealed clean cross-peaks between the *β*-H and N-H proton signals leading us to suggest that, in accord with the predictions by Gouterman *et al.*,[18] compounds **1**-**5** exist in one tautomeric form (Figure S41-S50).

X-ray Crystallography

Slow diffusion of n-hexane into $CHCl_3$ or CH_2Cl_2 solutions of *cis*/*trans* **3**-**5** provided single crystals suitable for X-ray diffraction analysis. The resulting crystal structures of *cis*/*trans*-**3** (CCDC nos.: 1568750 and 1568751), *cis*/*trans*-**4** (CCDC nos.: 1841552 and 1841553) and *cis*/*trans*-**5** (CCDC nos.: 1851807 and 1851808), respectively, are shown in Figure 2. Collectively, these structures provide support for the chemical assignments made initially on the basis of the spectroscopic and mass spectrometric analyses (vide supra), in particular the presence of a fused five-member ring on porphodilactone *β*-periphery in all six compounds (Table S1-S3 and Figure S51-S56). In **3**, the N-CH_3 moiety was found slanted towards the porphyrin ring in the *cis* isomer, while it was found to point in the opposite direction in the case of the *trans* isomer. The pyrrole-fused *β*-rings of *cis*/*trans*-**4** and the pyrrolidine-2,5-dione-fused *β*-rings of *cis*/*trans*-**5** were found to be coplanar with the porphyrin ring. The average C-N and C-C bond lengths are similar in *cis*/*trans*-**3**-**5** (Table S4-S6), a finding we take as meaning that are apart from the position of the substituents there are relatively small structural differences between the *cis* and *trans*-isomers. Across the series, both the *cis* and *trans* forms of **3**-**5** display relatively planar core porphyrinoid structures (RMSD = 0.072 and 0.104 Å for *cis*/*trans*-**3**, 0.085 and 0.161 Å for *cis*/*trans*-**4**, and 0.153 and 0.168 Å for *cis*/*trans*-**5**, respectively. Figure 2b).[12a, 19] Again, this is consistent with the suggestion that the key 1,3-dipolar cycloaddition that provides an entry into this series of porphyrinoids affects only slightly the planarity and configuration of the central macrocycle.

Photophysical Properties

The absorption and emission spectra of *cis*/*trans* **2**-**5** were recorded in CH_2Cl_2 at room temperature (Figure 3). The corresponding photophysical data are summarized in Table S7 and Figures S57-76. As can been seen from an inspection of Figure 3, all members of the *cis*/*trans* **2**-**5** series display intense Soret bands in the 350-450 nm spectral region, as well as several weak and broad Q bands at lower energy (between 450 and 780 nm). Compared with *cis*/*trans*-**1**, which displays typical bacteriochlorin absorption features,[3a, 3b] the lowest Q band of *cis*/*trans*-**2** are bathochromically shifted (by ca. 65 and 74 nm for the *cis* and *trans* isomers, respectively; cf. Table S7). *Cis*-**3** is characterized by a large hypsochromic shift in its Q bands (by ca. 108 nm) relative to *cis*-**1**, while only a smaller hypsochromic shift (by ca.

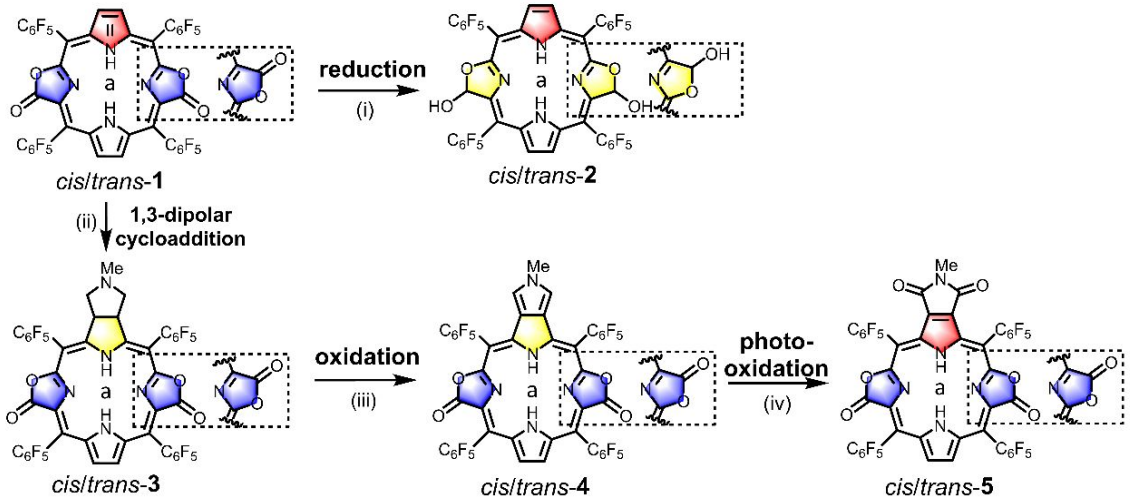

Scheme 1. Synthesis of *cis*/*trans*-**2**-**5**. Reagents and conditions: (i) DIBAL-H, THF, -78 ℃; (ii) sarcosine, paraformaldehyde, 105 ℃, toluene, 12 h; (iii) DDQ, toluene, reflux for 4 h; (iv) O_2, $CHCl_3$, irradiated under white light for 4 h.

Journal Name

ARTICLE

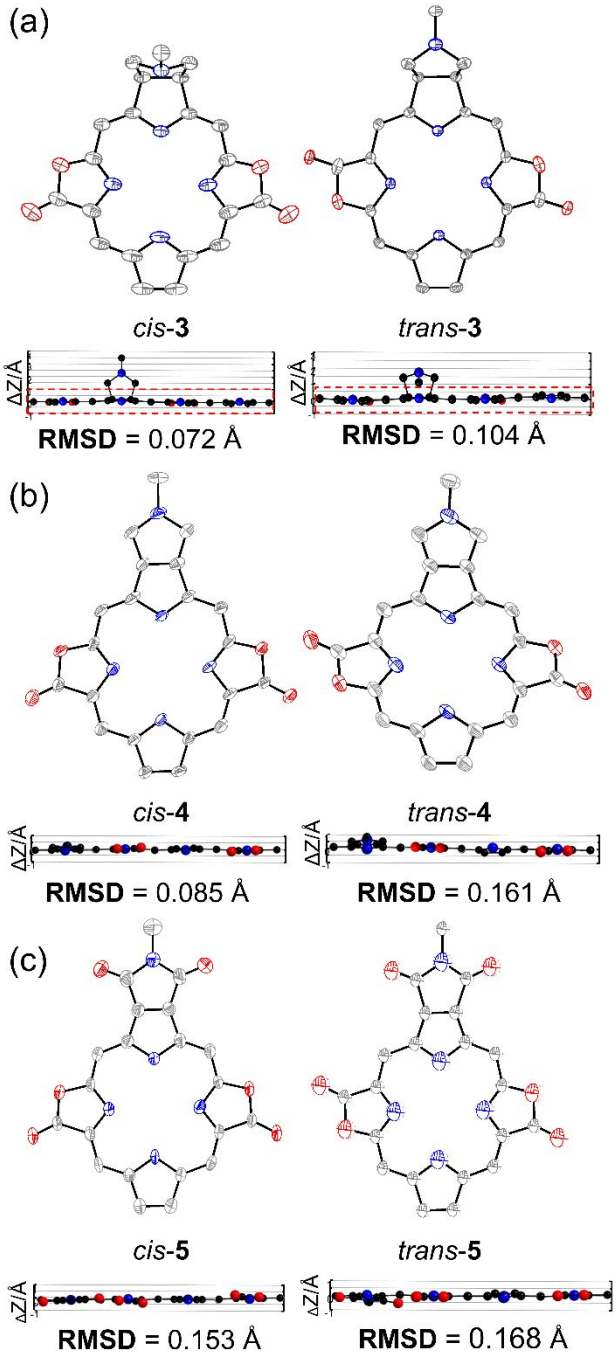

Figure 2. ORTEP structures of (a) *cis*/*trans*-**3**, (b) **4**, and (c) **5** (50% probability) showing the deviations of the skeletal atoms from the N_4 mean plane defined by the four pyrrolic nitrogen atoms. The RMSD values listed are of the $C_{18}O_4N_4$ ring (atoms shown within the red dashed line box). Hydrogen atoms, solvent molecules, and *meso*-aryl groups are omitted for clarity.

56 nm) is seen in the case of *trans*-**3** relatives to *trans*-**1**. *Cis* and *trans*-**4** both display bathochromically shifted Q-band features as compared to **1**. In contrast to the general trend of the *trans*-isomers showing red-shifted Q bands to their *cis* counterparts (as seen in **1**-**4**), *cis*-**5** is characterized by Q bands that are red-shifted relative to those seen in *trans*-**5** (Figure 3d). Taken in concert, the observed spectroscopic features, including the presence of prominent Soret and Q bands, leads us to suggest that aromaticity is retained in *cis*/*trans*-**1**-**5** in spite of the obvious structural modifications.[13d, 20] The increase in the value of ΔQ_Ls for the two isomers follows the trend: **1** (19 nm)[10a] ≈ **5** (20 nm) < **2** (28 nm) < **3** (71 nm) ≈ **4** (73 nm). This leads us to conclude that increasing from two to three the number of saturated pyrroles in otherwise similar porphyrinoids leads to an enhanced regioisomeric effect on the absorption features. In other words, moving from a *cis* to a *trans* isomer has a relatively greater effect in the case of more highly reduced porphyrinoids. This trend is underscored by the fact unprecedentedly large ΔQ_Ls of ca. 71 and 73 nm were seen in the case of *cis*/*trans*-**3** and **4**, respectively. In addition, the absorption difference between the lowest Soret bands for the *cis* and *trans* isomers follows a similar trend, namely **1** (2 nm) < **2** (4 nm) and **5** (9 nm) (both with two saturated pyrroles) < **4** (16 nm) and **3** (20 nm) (three saturated pyrroles).

A regioisomeric effect on the fluorescence emission spectra was seen. The underlying photophysical data measured in CH_2Cl_2 are summarized in Figure 3 and in Table S7. The trends were found to parallel what was seen in the case of the absorption spectral studies. For instance, *cis*/*trans*-**2** were characterized by fluorescence emission features centred at 737 and 754 nm with a shoulder at 784 and 828 nm, respectively. These values are bathochromically shifted relative to *cis*/*trans*-**1**. Quantum yields (Φ) of 6.1% and 5.3% and lifetimes (τ) of 2.1 ns and 2.6 ns were obtained for, *cis*-**2** and *trans*-**2**, respectively. *Cis*-**3** displays an emission maximum at 559 nm with a shoulder at 604 nm (Φ = 35.1%,τ = 5.5 ns), while the emission maximum of *trans*-**3** is red-shifted to 635 nm with a shoulder at 683 nm (Φ = 24.5 %,τ = 5.1 ns). Thus, the difference in the emission maxima is 76 nm. *Cis*- and *trans*-**4** display fluorescence maxima centred at 617 and 692 nm with quantum yields of 36.3% and 15.2% and lifetime of 8.34 ns and 3.29 ns, respectively. *Cis*/*trans*-**5** display NIR fluorescence features centred at 728 nm and 707 nm with quantum yields of 20.9% and 28.0%, respectively. Thus, as true for the corresponding absorption spectra, a relatively small difference in the emission maxima of 21 nm was seen for these two isomers. On the basis of the crystal structures of **1**, and **3**-**5**, the regioisomeric effects on the fluorescence emission features are not considered to arise from distortions of the respective porphyrin planes since all species have relatively planar structures.[12a, 19]

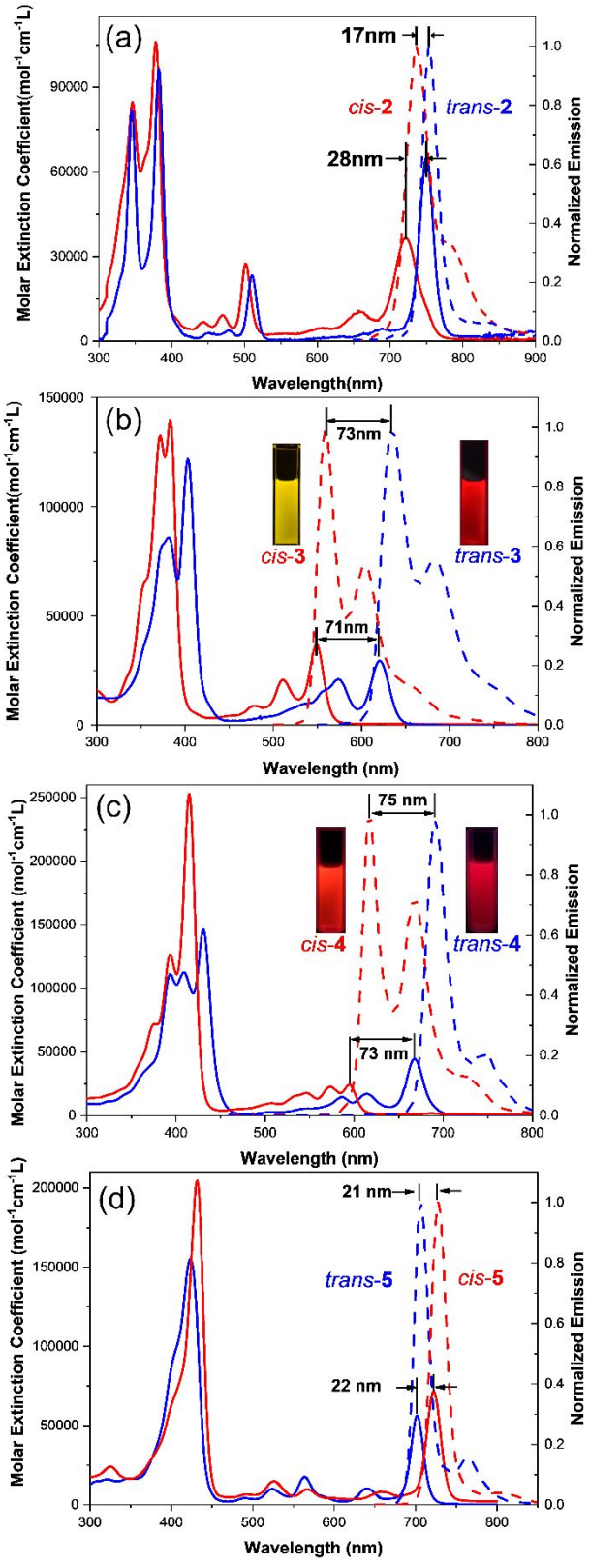

Figure 3. Electronic absorption (solid lines) and emission (dashed lines) spectra of (a) *cis*-**2** (red) and *trans*-**2** (blue), (b) *cis*-**3** (red) and *trans*-**3** (blue), (c) *cis*-**4** (red) and *trans*-**4** (blue) and (d) *cis*-**5** (red) and *trans*-**5** (blue) in CH_2Cl_2. Photographs of solutions of **3** and **4** taken under a 365 nm UV lamp are provided as inserts.

The redox properties of *cis*/*trans* **2**-**5** were examined in CH_2Cl_2 by cyclic voltammetry (CV) using tetra-n-butylammonium hexafluorophosphate (n-Bu_4NPF_6) as the supporting electrolyte. As shown in Table S7 and Figure S77-80, the CVs of *cis*/*trans*-**2**-**4** are each characterized by two quasi-reversible reduction waves and one quasi-reversible oxidation wave. In contrast, three quasi-reversible reduction waves are seen in the CVs of *cis*/*trans*-**5** and no oxidation waves were observed in CH_2Cl_2. The use of slower scan rate in the CV measurement studies failed to improve the reversibility of the redox waves (Figure S81 and Table S8), which was taken to indicate that the lack of reversibility is inherent to these tetrapyrroles, rather than the result of slow electron transfer kinetics at the electrode/electrolyte interface.

Modulating the Regioisomeric Effect by Aromaticity

Porphyrinoids **1**-**5** are expected to be aromatic compounds. Experimental support for this assumption comes from the observed the spectroscopic features, including the strong Soret bands, low field chemical shifts observed for the outer *β*-H protons (7.23-8.85 ppm), and the upfield shift seen for the inner pyrrole N-H protons (-2.12-6.53 ppm). However, the extent of aromaticity was expected to depend on the degree of unsaturation. Thus, we sought to test whether the optical features could be correlated with indicators of aromaticity. To the extent this proved true, it would provide an indication that differences in aromaticity could explain the large disparities in photophysical properties induced by ostensibly similar regioisomeric effects across the series of porphyrin analogues embodied in Figure 1.

Anisotropy of the induced current density (AICD) is a magnetic indicator of aromaticity that allows ring-currents and electron delocalization effects to be easily visualised.[21] As shown in Figure 4, AICD plots constructed at the B3LYP[22]/6-31+G(d) level[23] disclose ring circulation patterns typical of aromaticity across the series **1**-**5**. Reduction of **1** to **2** does not change the macrocyclic circulation within the porphyrin core but does reduce the ring current at the *β*-dilactol moieties. The 1,3-dipolar cycloaddition that serves to convert **1** into **3** acts to interrupt the circulation of one pyrrole ring and thus weaken the extent of aromaticity. In **3**, the lone pair of the pyrrollic N atom still participates in the π-conjugation pathway; thus **3** retains aromaticity. Oxidation of the pyrrolidine-fused *β*-rings in **3** to produce the pyrrole-fused *β*-rings present in *cis/trans*-**4** serves to restore partly the original level of aromaticity present in **1**. Presumably, this is due to the creation of a more extended π system but with a partially "broken" circulation. Photooxidation of **4** to **5** can completely restore the macrocyclic circulation as well as the aromaticity within the porphyrin rings. Thus, the AICD plots constructed at an isosurface value of 0.06 for **1**-**5** clearly show the changes of macrocyclic and local π circulation that result from *β*-modification. However, it is important to appreciate that in our hands this technique does not provide insights into the regioisomeric effect on macrocyclic π-conjugation.

In light of the above limitations, the isotropic nucleus-independent chemical shift (NICS)[24] values were calculated at the

Journal Name

ARTICLE

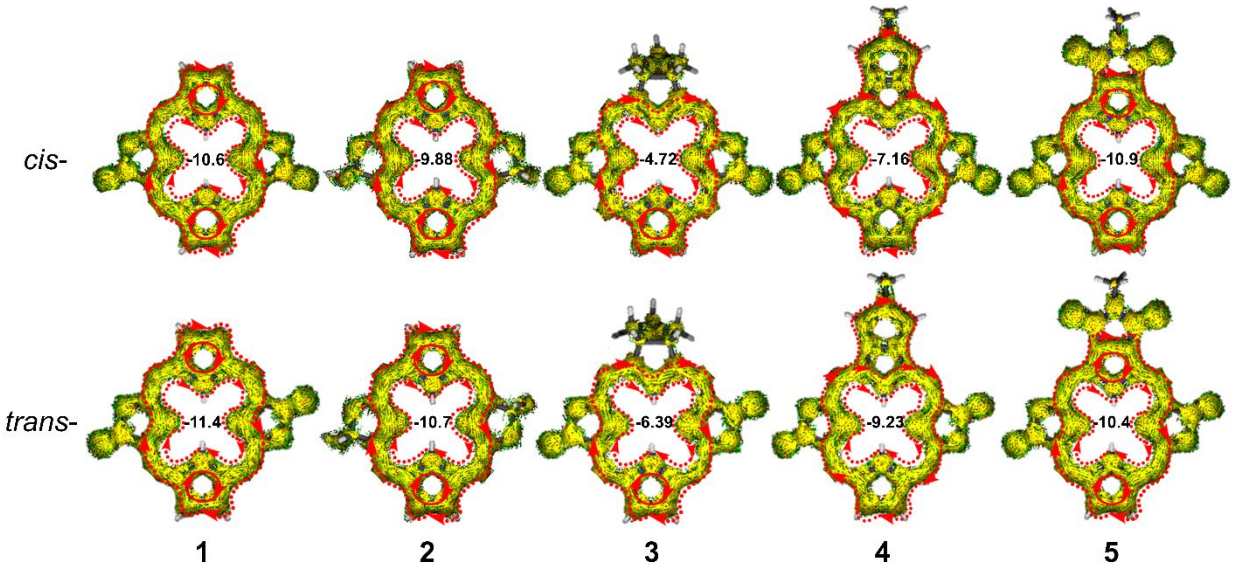

Figure 4. AICD plots at isosurface values of 0.06 and NICS(1) values (black number in the middle of molecules) calculated for *cis*/*trans* **1**-**5**.

Table 1. N-H pyrrolic proton chemical shifts, NICS(1) values and ΔQ_L of *cis/trans*-**1**-**5**.

Comp.		$\delta_{N\text{-}H}$/ppm	Avg. $\delta_{N\text{-}H}$[a] /ppm	NICS(1) /ppm	Avg. NICS(1)[b] /ppm	ΔQ_L /cm^{-1}
1	*cis*	-0.95, -0.33	-1.38	-10.61	-10.99	428
	trans	-2.12		-11.37		
2	*cis*	0.79, 1.26	-0.16	-9.88	-10.29	517
	trans	-1.35		-10.71		
3	*cis*	5.45, 6.53	4.90	-4.72	-5.56	2086
	trans	3.48, 4.13		-6.39		
4	*cis*	2.39, 3.51	1.72	-7.16	-8.19	1837
	trans	0.19, 0.79		-9.23		
5	*cis*	-1.05, -1.64	-1.01	-10.93	-10.65	395
	trans	-0.66, -0.69		-10.36		

[a]Avg. $\delta_{N\text{-}H} = [n_{cis}*(\delta_{N\text{-}H})_{cis} + n_{trans}*(\delta_{N\text{-}H})_{trans}] / (n_{cis} + n_{trans})$, where n is the integrated value of the N-H proton signal in the ^{1}H NMR spectra; [b]Avg. NICS(1) = [NICS(1)$_{cis}$ + NICS(1)$_{trans}$] / 2.

B3LYP/6-31+G(d) level so as to compare more quantitatively the aromaticity of *cis/trans*-**1**-**5**. In particular, the NICS(1) values of the ring a (Scheme 1) were determined, with the resulting findings being summarized in Tables 1 and S9. On this basis, it was concluded that within this matched set, whether considering the *cis*- or *trans*-isomer, the order of the NICS(1) values increases in the order **1**~**5**< **2**<**4**<**3**. This trend is in the line with what is seen for the chemical shifts of the inner N-H protons (-2.12-6.53 ppm) or those of the outer *β*-H signals (7.23-8.85 ppm).

To verify the validity of computational work, we correlated the chemical shifts of the N-H proton signals for all compounds in the study, as well as their average value for each isomeric pair, with the corresponding NICS(1) values.[25] Interestingly, plotting the NICS(1) values vs the chemical shifts of the pyrrole N-H proton signals produced a positive correlation (Figure 5a). Moreover, the NICS(1) values were found to be inversely correlated with the chemical shifts of the *β*-H protons (Figure S82). Interestingly, ΔNICS values of <2 ppm were seen between isomers. These differences were not significant enough to draw conclusions about differences in aromaticity between the *cis*/*trans*-isomers. On the other hand, with the exception of **5**, the *trans*-isomers are characterized by more negative NICS(1) values than the *cis*-isomers.

To probe a possible relationship between the regioisomeric effect and the aromaticity of porphyrinoids, we correlated ΔQ_Ls in units of energy (cm^{-1}) vs the aromaticity represented by the average NICS(1) values for **1**-**5**. As shown in Figure 5b, we obtained a positive correlation. In addition, we also plotted ΔQ_L values *vs* the average chemical shifts of the N-H (Figure S83) and the *β*-H proton signals (Figure S84), as well as the Δ(Soret band) values *vs* the average NICS(1) values for **1**-**5** (Figure S85 and Table S10); the same trend was

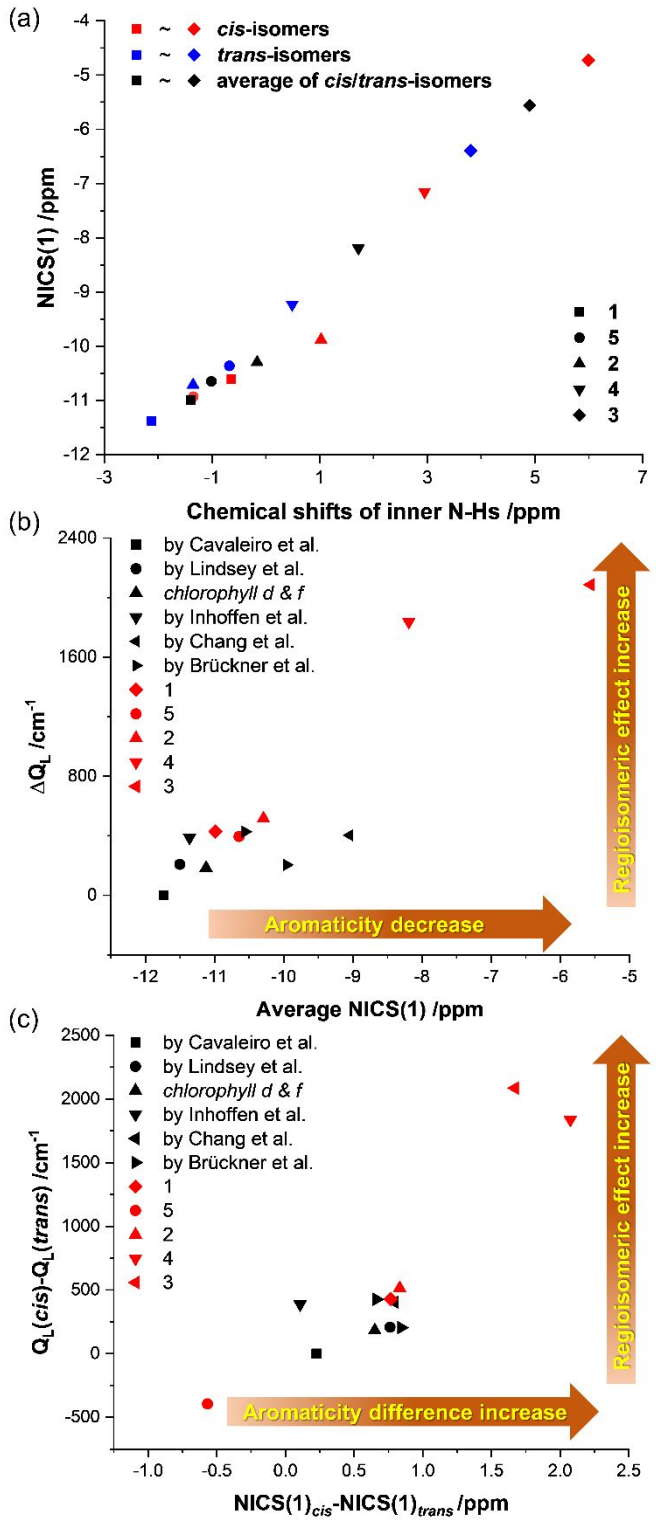

Figure 5. (a) Relationship between the calculated NICS(1) values *vs* chemical shifts of the inner N-H proton signals observed in the ^{1}H NMR spectra of **1**-**5**. (b) Plot of a key photophysical parameter (ΔQ_L) *vs* aromaticity as inferred from the NICS(1) values and (c) plot of regioisomeric effect (Q_L(*cis*)-Q_L(*trans*)) *vs* aromaticity difference between *cis* and *trans* isomers (NICS(1)$_{cis}$-NICS(1)$_{trans}$) for compounds **1**-**5** (red) and seven other previously reported isomeric pairs (black) discussed in the Introduction.

observed. Again, these plots help underscore the fact that the regioisomeric substitution effects that are well appreciated for chlorophylls can be enhanced significant in the case of more highly unsaturated systems. For example, on passing from **3** to **5** via the chemistry outlined in Scheme 1, a significant change in the magnitude of the regioisomeric effect on ΔQ_L is seen. Moreover, the nearly linear plotting of regioisomeric effect (Q_L(*cis*)-Q_L(*trans*)) *vs* aromaticity difference between *cis* and *trans* isomers (NICS(1)$_{cis}$-NICS(1)$_{trans}$) for compounds **1**-**5** and seven other previously reported isomeric pairs (Figure 5c) further indicates that the enlarged regioisomeric effects on photophysical properties originate from the increased aromaticity difference between isomers.

Electronic Structures

To investigate the regioisomeric effect on the electronic structures of **1**-**5**, density functional theory (DFT) calculations were performed at the B3LYP/6-31+G(d) level. Based on the 2D NMR spectroscopic studies noted above, we discounted the possibility of tautomerism involving the N-H protons within the N_4 cavity and considered only the tautomers where these protons were located on the pyrrolic moieties.[18] The nodal patterns of the frontier molecular orbitals (FMOs) and the corresponding energy diagrams were then derived in accord with Gouterman's four-orbitals model.[26] The results are shown in Figure 6. From 5,10,15,20-*tetrakis*(perfluorophenyl)-porphyrin (F20-porphyrin) to **1**-**5**, the energy levels of the HOMOs and LUMOs decrease, as expected given the strong electron-withdrawing nature of the *β*-diazalone moiety. As a result, the HOMO-LUMO gap (HL gap) decreases from 2.80 eV in F20-porphyrin to 2.46 and 2.34 eV in *cis*- and *trans*-**1**, respectively. From **1** to **2**, the HOMO-LUMO gap (HL gap) of the *cis*- and *trans* isomers decreases further to 2.09 and 2.01 eV, respectively, presumably due to the further decrease in the orbital degeneracy that occurs upon reduction of the *β*-diazalone to the corresponding dilactol moieties. This reduction in the HL gap is also in accord with the bathochromic shifted Q_L bands seen for **2** relatives to **1** and the other systems under study. For *cis*-**3**, the energy of LUMO increases more than that of HOMO, leading to an increased HL energy gap (2.64 eV) compared with *cis*-**1** (2.46 eV).[10a] In contrast, the HL energy gap of *trans*-**3** (2.35 eV) is almost the same as that of *trans*-**1** (2.34 eV).[10a] Therefore, it is not surprising that a much larger ΔQ_L between the *cis*/*trans* isomers is seen in the case of **3** than in **1**. The HL gap is almost the same for *cis*-**3** (2.64 V) and *cis*-**4** (2.67 eV), a finding that reflects the nearly identical energy changes in the HOMO and LUMO energies for these two systems. The HOMO energy of *trans*-**3** is higher in energy level than that of *trans*-**4**; this is reflected in a decrease in the HL energy gap (from 2.35 to 2.26 eV) upon conversion of **3** to **4**. The HOMO energies of *cis*/*trans*-**5** are the lowest within the series **1**-**5**. Such a finding is consistent with the relatively anodic oxidation waves seen in the electrochemical measurements. The nearly linear relationship of HL gap *vs* observed Q band, calculated Q band vs experimental Q band and ΔHOMO vs oscillator strengths in TDDFT calculations validate our calculation results according Martin J. Stillman et al (Figure S86-S88).[27] Thus, overall the HL gaps seen for **1**-**5** follow the

Journal Name

ARTICLE

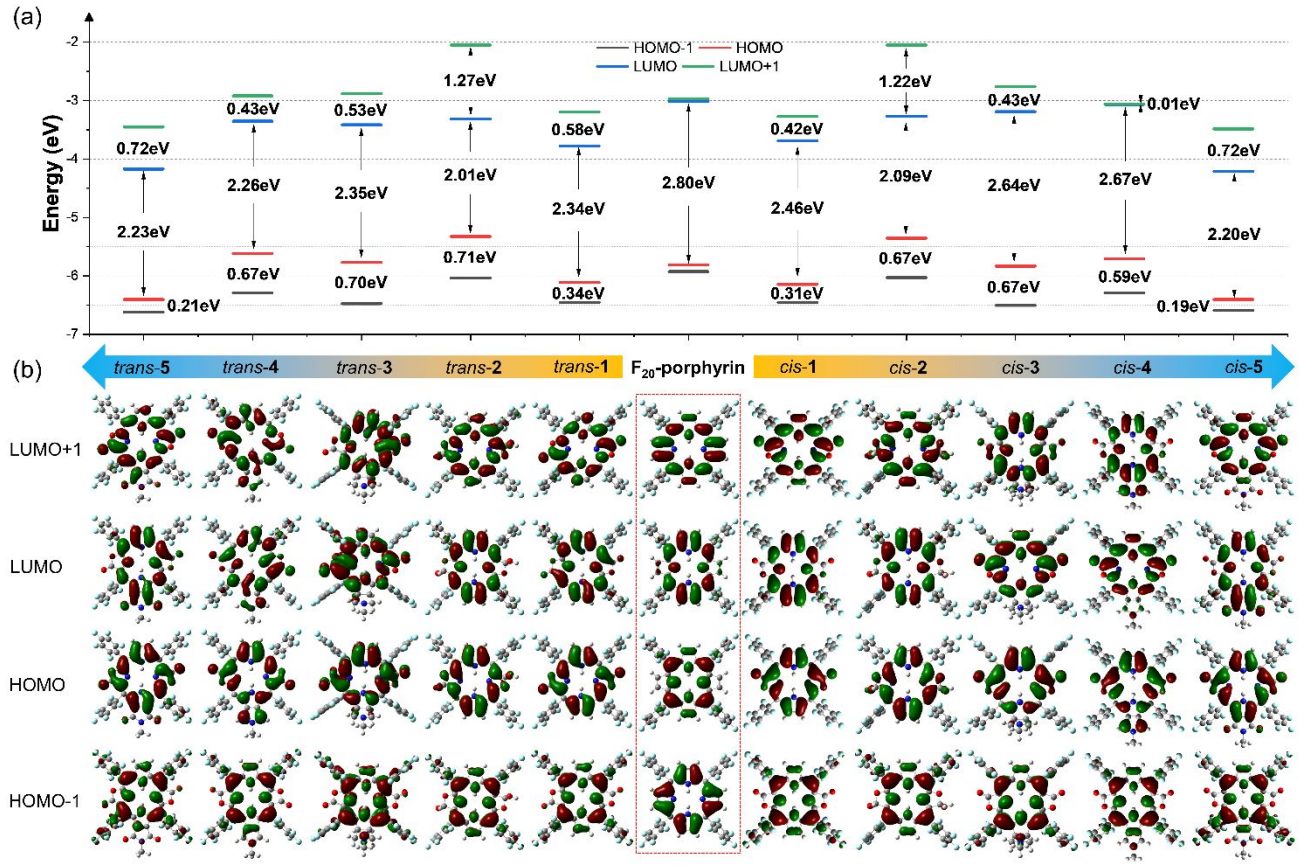

Figure 6. (a) Energies of selected molecular orbitals of *cis*/*trans*-**1**-**5** as determined by DFT calculations carried out at the B3LYP/6-31+G(d) level. (b) Nodal patterns of the frontier π-MOs of *cis*/*trans*-**1**-**5** calculated using the optimized S_0 geometries.

trend for the $Q_L(0,0)$ bands discussed above (Figure S89). They thus provide another indicator of the effect of porphyrin periphery saturation on the electronic structure of these reduced porphyrinoids. This correspondence between theory and experiment also serves to validate our DFT calculations.

As shown in Figure 6b, the HOMO–1 frontier orbitals in **1**-**5** resemble the Gouterman a_{1u} orbitals modified for the presence of strongly electron-withdrawing diazalone moieties. Likewise, the HOMO frontier orbitals in **1**-**5** resemble the Gouterman a_{2u} orbitals. In contrast, the HOMO-1 and HOMO orbitals of **1**-**5** are different from the corresponding orbitals in F20-porphyrin.[26a, 28] The LUMO and LUMO+1 orbitals for **1**-**5** resemble Gouterman's e_g orbitals oriented along two opposite pyrrolic fragments.[26a, 28] For F20-porphyrin, as well as **1**-**2** and **5**, the lower energy LUMO is oriented along the axis of the pyrrolic ring containing the inner N-H bonds. In the case of **3** and **4**, the lower energy LUMO within the Gouterman e_g set is oriented toward the *β*-diazalone moieties. Thus, *β*-modification significantly decreases the degeneracy of the FMOs in **1**-**5**, presumably due to the reduction in symmetry (from D_{2h} to C_{2v} for the *cis* isomers, and from D_{2h} to C_{2h} or C_s for the *trans* isomers) compared with the control F20-porphyrin system.[28]

Magnetic circular dichroism (MCD) spectroscopy can provide information about molecular electronic structure and electronic transitions that complements that obtained from absorption and emission spectroscopy.[29] Therefore, the MCD spectra of **1**-**5** were recorded as shown in Figure 7. The nodal patterns of the frontier π-MOs are maintained even after substantial structural perturbations as shown in Figure 6b and can, therefore, be related back to those of an ideal high symmetry parent hydrocarbon ($C_{18}H_{18}$ for free base compounds).[29a] According to Michl's perimeter model,[29a, 30] in high symmetry cyclic polyenes, the π-MOs associated with the perimeter retain orbital degeneracy described by the Faraday A_1, B_0 and C_0 terms. Typically, positive Faraday A_1 terms are the dominant spectral feature since the orbital angular momentum associated with the LUMO is usually higher than that associated

Journal Name

ARTICLE

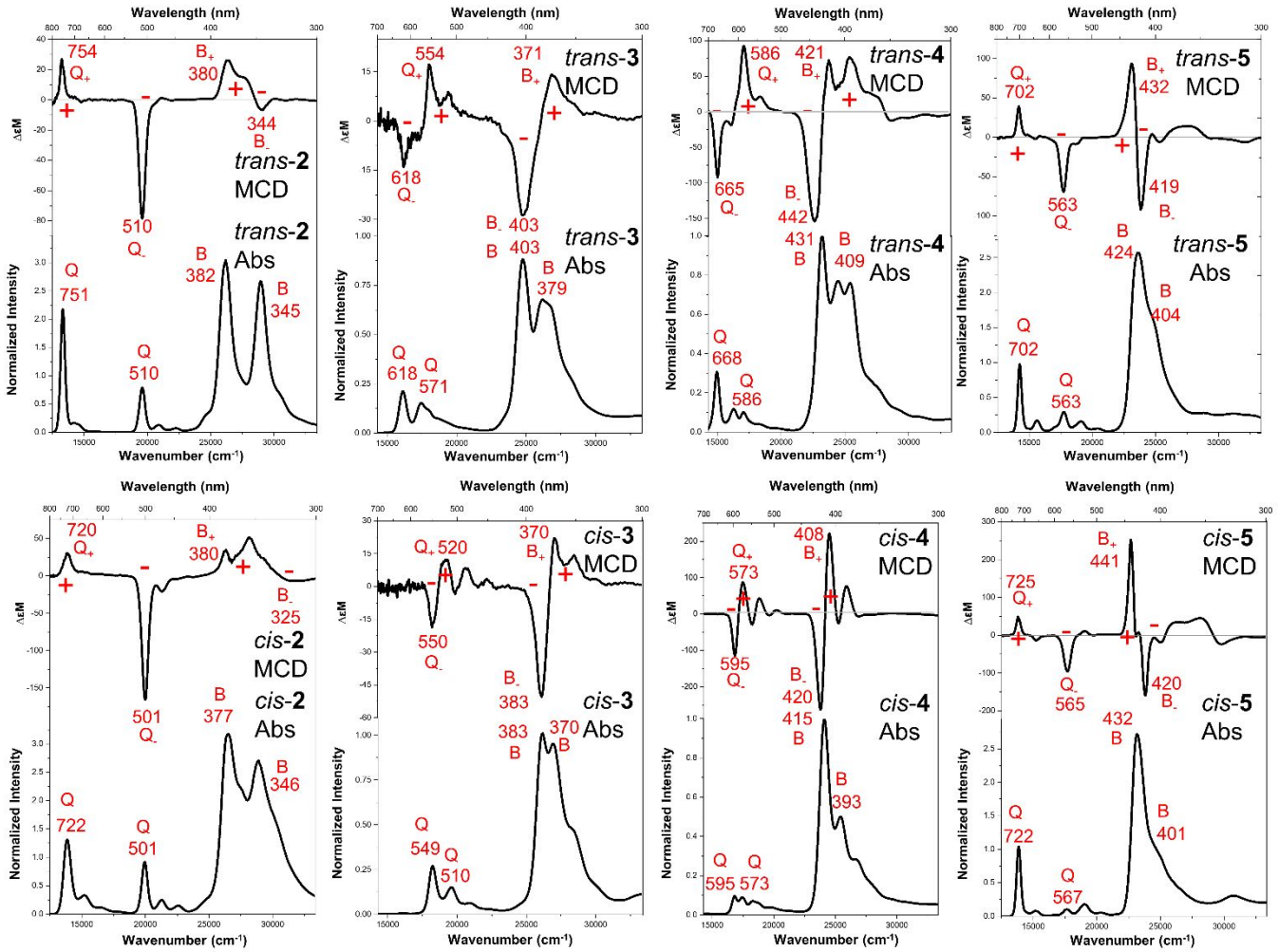

Figure 7. MCD (top) and normalized electronic absorption (bottom) of *cis*/*trans* **2-5** in CH_2Cl_2 at room temperature.

with the HOMO.[29a] When the symmetry of the cyclic perimeter is modified, a lifting of the orbital degeneracy of the HOMOs or the LUMOs occurs and the A_1 terms of high symmetry complexes are replaced by coupled oppositely signed B_0 terms with the same basic −ve/+ve or +ve/−ve sign sequence.[29a] In reduced symmetry porphyrinoids, the Q band ($\Delta M_L = \pm 1$) and B band ($\Delta M_L = \pm 9$) transitions tend to have the strongest magnetic transition dipole moments and, therefore, are most extensively mixed by the applied field.[29a, 30] Consequently, the alignment of the magnetic moment is determined by the relative energy separations of the frontier π-MOs derived from the HOMO and LUMO (ΔHOMO, ΔLUMO) of the parent hydrocarbon perimeter.[30b] In porphyrinoids with ΔHOMO ≈ ΔLUMO, systems referred to as soft MCD chromophores by Michl,[29a] small structural changes can reverse the direction of the induced magnetic dipole excited states. When ΔHOMO > ΔLUMO, the orbital angular momentum associated with the excited electron predominates and there is a −ve/+ve/−ve/+ve intensity pattern (manifest as a "-, +, -, +" ordering in signal signs for the Q and B bands) with an ascending energy for the Faraday B_0 terms associated with Platt's L (Q) and B bands.[29a, 31] When ΔLUMO > ΔHOMO, the sign sequence for the Faraday B_0 terms in ascending energy becomes +ve/−ve/+ve/−ve (i.e., an ordering of "+, -, +, -" in the signal signs for the Q and B bands).[29a, 31b] As shown in Figure 5, an ordering of "+, −, +, −" is seen in the MCD spectra of *cis*/*trans*-**2** and **5** in accord with the calculated ΔHOMO < ΔLUMO. Likewise, the observed ordering of "−, +, −, +" in the MCD spectra of **3** and **4** is also consistent with the calculations, namely ΔHOMO > ΔLUMO. The fact that the sign sequences observed in the MCD spectra for the B_0 terms associated with the Q and B bands are broadly consistent with the trends that would be anticipated based on the MO energies predicted in the B3LYP geometry optimizations

is taken as further validation of the theoretical descriptions used to define the electronic structures of *cis*/*trans*-**2**-**5**.

As may be inferred from Figure 6 and in accord with Gouterman's four orbital model,[26] the regioisomeric effect on the electronic structures has its origins in the energy level splitting of the FMOs associated with each given pair of regioisomers. Within the series **1**-**5**, the *trans*-isomers stabilize a_{1u} orbitals and destabilize a_{2u} orbitals to a greater extent than the *cis*-isomers. Therefore, the ΔHOMOs for the *trans*-isomer are generally larger than those for the corresponding *cis*-isomers. Similarly, the *trans*-isomers are characterized by LUMO energies that are relatively lowered more than the corresponding LUMO+1 orbitals. They thus have larger ΔLUMOs than their *cis*-counterparts (note, however, that the ΔLUMOs of *cis*/*trans*-**5** are the same). On this basis, we conclude that the observed regioisomeric effects on the photophysical properties, including the ΔQ_Ls, are dependent on the HL gaps but are essentially tied to the degeneracy and energy level splitting of the FMOs.

Conclusions

Reported here is a series of porphodilactones derivatives (*cis*/*trans*-**2**-**5**) that differ in terms of the extent and nature of the saturation associated with porphyrin periphery. Specifically, by means of *β*-diazalone reduction or 1,3-dipolar cycloaddition, a congruent set of relatively reduced regioisomers was obtained. The regioisomeric effect of substitution was readily apparent in terms of readily measured spectroscopic features. For instance, the ΔQ_L values vs were found to follow the trend *cis*/*trans*-**1** (19 nm)[10a] ≈ *cis*/*trans*-**5** (22 nm) < **2** (28 nm) < **3** (71 nm) ≈ **4** (73 nm) for ΔQ_Ls. Importantly, the degree of modulation within this series was much larger than what might be interpolated from corresponding studies with chlorophyll derivatives. AICD plots at iso-surface values of 0.06 and the calculated NICS (1) values revealed a correlation between the specifics of the porphyrin periphery and the global aromaticity of the system in question. The chemical shift values of the inner N-H protons in the ^{1}H NMR spectrum also proved well correlated with the calculated NICS (1) values. Experimental (MCD and ^{1}H-NMR spectra) and theoretic studies based on DFT calculation on the level of B3LYP/6-31+G(d) allowed the effect of saturation around the porphyrin periphery to be correlated to the degree of frontier molecular orbital (FMO) splitting.

On the basis of the observed effects and the strong interplay between structure and optical effects, we suggest that in porphyrinoids, a close relationship is expected to exist between the degree of *β*-pyrrolic saturation and aromaticity just as it can for *meso*-substitution.[32] The effect of *β*-pyrrolic saturation further depends on regioisomeric differences as illustrated by the present analysis of the photophysical properties of a set of reduced, aromatic porphyrinoids, namely *cis*/*trans*-**1**-**5**, as well as consideration of four previously reported isomeric systems introduced by Chang and Brückner.[7, 10b] Specifically, an effect that is barely noticeable in the case of porphyrins, discernible but small in the case of chlorophylls and related systems, becomes exceptionally large as the degree of *β*-pyrrolic saturation (and hence global aromaticity) is further reduced (cf. Figure 1). This unexpected finding sets the stage for the design of new porphyrinoid-based functional materials whose photophysical features are fine-tuned via subtle structural changes.

Conflicts of interest

No competing financial interests have been declared.

Acknowledgements

We thank Prof. M. J. Stillman for his useful suggestion and discussion regarding the DFT and TDDFT calculation. We acknowledge financial support from the National Key Basic Research Support Foundation of China (Grant 2015CB856301) and the National Scientific Foundation of China (Grants 21778002, 21571007, 21271013, 21321001). This work was supported by the High-performance Computing Platform of Peking University. Support from the Robert A. Welch Foundation (F-0018 to J.L.S.), the U.S. National Science Foundation (CHE-1807152 to J.L.S.) and Shanghai University is also acknowledged.

Notes and references

1. a) M. Schliep, G. Cavigliasso, R. G. Quinnell, R. Stranger and A. W. Larkum, *Plant Cell Environ.*, 2013, **36**, 521-527; b) M. Chen, *Annu. Rev. Biochem.*, 2014, **83**, 317-340; c) L. O. Björn and H. Ghiradella, in *Photobiology*, 2015, DOI: 10.1007/978-1-4939-1468-5_9, ch. Chapter 9, pp. 97-117; d) Z. Zhou and Z. Shen, *Isr. J. Chem.*, 2016, **56**, 119-129; e) M. Taniguchi and J. S. Lindsey, *Chem. Rev.*, 2017, **117**, 344-535; f) G. N. Lewis and Melvin. Calvin, *Chem. Rev.*, 1939, **25** 273–328.
2. a) J. E. Coughlin, Z. B. Henson, G. C. Welch and G. C. Bazan, *Acc. Chem. Res.*, 2014, **47**, 257-270; b) C. Zhang, Y. Zang, F. Zhang, Y. Diao, C. R. McNeill, C. A. Di, X. Zhu and D. Zhu, *Adv. Mater.*, 2016, **28**, 8456-8462; c) H. Huang, L. Yang, A. Facchetti and T. J. Marks, *Chem. Rev.*, 2017, **117**, 10291-10318; d) Y. Li, D. H. Lee, J. Lee, T. L. Nguyen, S. Hwang, M. J. Park, D. H. Choi and H. Y. Woo, *Adv. Funct. Mater.*, 2017, **27**, 1701942; e) C. Zhang and X. Zhu, *Acc. Chem. Res.*, 2017, **50**, 1342-1350.
3. a) K. M. Kadish, K. M. Smith and R. Guilard, *The Porphyrin Handbook*, Academic Press, New York, 2000; b) H. Scheer, M. O. Senge, A. Wiehe, C. Ryppa, M. Zapata, J. L. Garrido, S. W. Jeffrey, M. Kobayashi, M. Akiyama and H. Kise, *Chlorophylls and Bacteriochlorophylls*, Springer Netherlands, 2006; c) J. K. Hoober, L. L. Eggink and M. Chen, *Photosynth. Res.*, 2007, **94**, 387-400; d) M. Chen and R. E. Blankenship, *Trends. Plant. Sci.*, 2011, **16**, 427-431; e) M. Y. Ho, G. Shen, D. P. Canniffe, C. Zhao and D. A. Bryant, *Science*, 2016, **353**, aaf9178; f) D. J. Nürnberg, J. Morton, S. Santabarbara, A. Telfer, P. Joliot, L. A. Antonaru, A. V. Ruban, T. Cardona, E. Krausz, A. Boussac, A. Fantuzzi and A. W. Rutherford, *Science*, 2018, **360**, 1210-1213.
4. M. Chen, M. Schliep, R. D. Willows, Z. L. Cai, B. A. Neilan and H. Scheer, *Science*, 2010, **329**, 1318.
5. a) M. Liu, M. Ptaszek, O. Mass, D. F. Minkler, R. D. Sommer, J. Bhaumik and J. S. Lindsey, *New J. Chem.*, 2014, **38**, 1717-1730; b) J. M. Yuen, M. A. Harris, M. Liu, J. R. Diers, C. Kirmaier, D. F. Bocian, J. S. Lindsey and D. Holten, *Photochem. Photobiol.*, 2015, **91**, 331-342.
6. H. H. Inhoffen and W. Nolte, *Eur. J. Org. Chem.*, 1969, **725**, 167-176.
7. C. K. Chang and W. Wu, *J. Org. Chem.*, 1986, **51**, 2134-2137.
8. M. Mylrajan, L. A. Andersson, T. M. Loehr, W. S. Wu and C. K. Chang, *J. Am. Chem. Soc.*, 1991, **113**, 5000-5005.

9. A. M. G. Silva, M. A. F. Faustino, T. M. P. C. Silva, M. G. P. M. S. Neves, A. C. Tome, A. M. S. Silva and J. A. S. Cavaleiro, *J. Chem. Soc., Perkin Trans. 1*, 2002, 1774-1777.
10. a) X. S. Ke, Y. Chang, J. Z. Chen, J. Tian, J. Mack, X. Cheng, Z. Shen and J.-L. Zhang, *J. Am. Chem. Soc.*, 2014, **136**, 9598-9607; b) J. Ogikubo, E. Meehan, J. T. Engle, C. J. Ziegler and C. Brückner, *J. Org. Chem.*, 2013, **78**, 2840-2852.
11. a) X. S. Ke, H. Zhao, X. Zou, Y. Ning, X. Cheng, H. Su and J.-L. Zhang, *J. Am. Chem. Soc.*, 2015, **137**, 10745-10752; b) X. S. Ke, Y. Ning, J. Tang, J. Y. Hu, H. Y. Yin, G. X. Wang, Z. S. Yang, J. Jie, K. Liu, Z. S. Meng, Z. Zhang, H. Su, C. Shu and J.-L. Zhang, *Chem. Eur. J.*, 2016, **22**, 9676-9686; c) Y. Ning, X. S. Ke, J. Y. Hu, Y. W. Liu, F. Ma, H. L. Sun and J.-L. Zhang, *Inorg. Chem.*, 2017, **56**, 1897-1905.
12. a) B. Roder, M. Buchner, I. Ruckmann and M. O. Senge, *Photochem. Photobiol. Sci.*, 2010, **9**, 1152-1158; b) H. Tamiaki, M. Xu and Y. Kinoshita, *J. Photoch. Photobio. A*, 2013, **252**, 60-68.
13. a) C. Leumann, K. Hilpert, J. Schreiber and A. Eschenmoser, *J. Chem. Soc. Chem. Comm.*, 1983, **23**, 1404-1407; b) R. Waditschatka, E. Diener and A. Eschenmoser, *Angew. Chem. Int. Ed.*, 1983, **22**, 631-632; c) C. Leumann and A. Eschenmoser, *J. Chem. Soc. Chem. Comm.*, 1984, **9**, 583-585; d) A. M. Silva, A. C. Tomé, M. G. Neves, A. M. Silva and J. A. Cavaleiro, *J. Org. Chem.*, 2005, **70**, 2306-2314.
14. Y. Yu, H. Lv, X. Ke, B. Yang and J.-L. Zhang, *Adv. Synth. Catal.*, 2012, **354**, 3509-3516.
15. D. Park, S. D. Jeong, M. Ishida and C. H. Lee, *Chem. Commun.*, 2014, **50**, 9277-9280.
16. C. M. Carvalho, M. G. Neves, A. C. Tome, F. A. Paz, A. M. Silva and J. A. Cavaleiro, *Org. Lett.*, 2011, **13**, 130-133.
17. C. Brückner, J. R. McCarthy, H. W. Daniell, Z. D. Pendon, R. P. Ilagan, T. M. Francis, L. Ren, R. R. Birge and H. A. Frank, *Chem. Phys.*, 2003, **294**, 285-303.
18. a) M. Gouterman, R. J. Hall, G.-E. Khalil, P. C. Martin, E. G. Shankland and R. L. Cerny, *J. Am. Chem. Soc.*, 1989, **111**, 3702-3707; b) H. García-Ortega, J. Crusats, M. Feliz and J. M. Ribó, *J. Org. Chem.*, 2002, **67**, 4170-4176.
19. M. J. Guberman-Pfeffer, J. A. Greco, L. P. Samankumara, M. Zeller, R. R. Birge, J. A. Gascon and C. Brückner, *J. Am. Chem. Soc.*, 2017, **139**, 548-560.
20. J. E. Johansen, V. Piermattie, C. Angst, E. Diener, C. Kratky and A. Eschenmoser, *Angew. Chem. Int. Ed.*, 1981, **20**, 261-263.
21. a) R. Herges and D. Geuenich, *J. Phys. Chem. A*, 2001, **105**, 3214-3220; b) D. Geuenich, K. Hess, A. Felix Köhler and R. Herges, *Chem. Rev.*, 2005, **105**, 3758-3772; c) Y. Chang, H. Chen, Z. Zhou, Y. Zhang, C. Schütt, R. Herges and Z. Shen, *Angew. Chem. Int. Ed.*, 2012, **51**, 12801–12805; d) J. I. Wu, I. Fernández and P. v. R. Schleyer, *J. Am. Chem. Soc.*, 2013, **135**, 315-321.
22. a) C. Lee, W. Yang and R. G. Parr, *Phys. Rev. B: Condens. Matter Mater. Phys.*, 1988, **37**, 785–789; b) A. D. Becke, *J. Chem. Phys.*, 1993, **98**, 5648–5652; c) A. Dreuw and M. Head-Gordon, *J. Am. Chem. Soc.*, 2004, **126**, 4007-4016.
23. a) P. C. Hariharan and J. A. Pople, *Theor. Chim. Acta*, 1973, **28**, 213-222; b) M. M. Francl, W. J. Petro, W. J. Hehre, J. S. Binkley, M. S. Gordon, D. J. DeFree and J. A. Pople, *J. Chem. Phys.*, 1982, **77**, 3654-3665.
24. a) P. v. R. Schleyer, C. Maerker, A. Dransfeld, H. Jiao and N. J. R. van Eikema Hommes, *J. Am. Chem. Soc.*, 1996, **118**, 6317-6318; b) P. von Ragué Schleyer, H. Jiao, N. J. R. van Eikema Hommes, V. G. Malkin and O. L. Malkina, *J. Am. Chem. Soc.*, 1997, **119**, 12669-12670.
25. a) J. A. Gomes and R. B. Mallion, *Chem. Rev.*, 2001, **101**, 1349-1383; b) R. H. Mitchell, *Chem. Rev.*, 2001, **101**, 1301–1316.
26. a) M. Gouterman, *J. Chem. Phys.*, 1959, **30**, 1139-1161; b) M. Gouterman, ed. D. Dolphin, Academic Press, New York, 1978, vol. 3, ch. Part A, p. 1−165.
27. a) J. Mack, Y. Asano, N. Kobayashi and M. J. Stillman, *J. Am. Chem. Soc.*, 2005, **127**, 17697-17711; b) A. Zhang, L. Kwan and M. J. Stillman, *Org. Bio. Chem.*, 2017, **15**, 9081-9094; c) A. Zhang and M. J. Stillman, *Phys. Chem. Chem. Phys.*, 2018, **20**, 12470-12482.
28. M. O. Senge, A. Ryan, K. Letchford, S. MacGowan and T. Mielke, *Symmetry*, 2014, **6**, 781-843.
29. a) J. Mack, M. J. Stillman and N. Kobayashi, *Coord. Chem. Rev.*, 2007, **251**, 429-453; b) N. Kobayashi, A. Muranaka and J. Mack, *Circular Dichroism and Magnetic Circular Dichroism Spectroscopy for Organic Chemists*, Royal Society of Chemistry, London, 2011.
30. a) J. Michl, *J. Am. Chem. Soc.*, 1978, **100**, 6812-6818; b) J. Michl, *J. Am. Chem. Soc.*, 1978, **100**, 6801–6811; c) J. Michl, *Pure Appl. Chem.*, 1980, **52**, 1549-1563.
31. a) J. R. Platt, *J. Chem. Phys.* , 1949, **17**, 484-495; b) H. M. Rhoda, J. Akhigbe, J. Ogikubo, J. R. Sabin, C. J. Ziegler, C. Bruckner and V. N. Nemykin, *J. Phys. Chem. A*, 2016, **120**, 5805-5815.
32. a) A. Y. O'Brien, J. P. McGann and G. R. Geier, 3rd, *J. Org. Chem.*, 2007, **72**, 4084-4092; b) A. J. Pistner, G. P. Yap and J. Rosenthal, *J. Phys. Chem. C*, 2012, **116**, 16918-168924; c) A. J. Pistner, D. A. Lutterman, M. J. Ghidiu, Y. Z. Ma and J. Rosenthal, *J. Am. Chem. Soc.*, 2013, **135**, 6601-6607; d) A. M. Bruce, E. S. Weyburne, J. T. Engle, C. J. Ziegler and G. R. Geier, 3rd, *J. Org. Chem.*, 2014, **79**, 5664-5672; e) A. J. Pistner, D. A. Lutterman, M. J. Ghidiu, E. Walker, G. P. Yap and J. Rosenthal, *J. Phys. Chem. C*, 2014, **118**, 14124-14132; f) J. Nieto-Pescador, B. Abraham, A. J. Pistner, J. Rosenthal and L. Gundlach, *Phys. Chem. Chem. Phys.*, 2015, **17**, 7914-7923; g) D. Kim, H. J. Chun, C. C. Donnelly and G. R. Geier, 3rd, *J. Org. Chem.*, 2016, **81**, 5021-5031.